



**HAL**  
open science

## Path planning of a laser-scanner with the control of overlap for 3d part inspection

Nguyen Duy Minh Phan, Yann Quinsat, Sylvain Lavernhe, Claire Lartigue

► **To cite this version:**

Nguyen Duy Minh Phan, Yann Quinsat, Sylvain Lavernhe, Claire Lartigue. Path planning of a laser-scanner with the control of overlap for 3d part inspection. 11th CIRP Conference on Intelligent Computation in Manufacturing Engineering, CIRP ICME'17 , 2017, Naples, France. hal-01654044

**HAL Id: hal-01654044**

**<https://hal.science/hal-01654044>**

Submitted on 4 Dec 2017

**HAL** is a multi-disciplinary open access archive for the deposit and dissemination of scientific research documents, whether they are published or not. The documents may come from teaching and research institutions in France or abroad, or from public or private research centers.

L'archive ouverte pluridisciplinaire **HAL**, est destinée au dépôt et à la diffusion de documents scientifiques de niveau recherche, publiés ou non, émanant des établissements d'enseignement et de recherche français ou étrangers, des laboratoires publics ou privés.

# Path planning of a laser-scanner with the control of overlap for 3d part inspection

Nguyen Duy Minh Phan<sup>a</sup>, Yann Quinsat<sup>a,\*</sup>, Sylvain Lavernhe<sup>a</sup>, Claire Lartigue<sup>a</sup>

<sup>a</sup>LURPA, ENS Paris-Saclay, Univ. Paris-Sud, Université Paris-Saclay, 61 Avenue du Président Wilson, 94235 Cachan, France

\* Corresponding author. Tel.: +33-147-402-213; fax: +33-147-402-220. E-mail address: yann.quinsat@ens-paris-saclay.fr

---

## Abstract

This paper proposes a new approach to scan path planning for automated inspection of manufactured parts with an industrial robot based on the control of the overlap between 2 successive scanning paths. The novelty lies in the use of the least-squares conformal map, which stretches a 3D surface on a 2D plane. Equidistant paths calculated in the 2D space are transformed into equidistant paths in the 3D space. Controlling the overlap can maximize the coverage region on the scanned part. On the other hand, digitizing quality is ensured by managing the sensor configuration relatively to the part with respect to quality criteria. The approach is implemented with success for a laser-plane scanner mounted on an industrial robot.

© 2017 The Authors. Published by Elsevier B.V.

Peer-review under responsibility of the scientific committee of the 11th CIRP Conference on Intelligent Computation in Manufacturing Engineering.

*Keywords:* Inspection; Scan path, Overlap; Least squares conformal maps; Robot

---

## 1. Introduction

In the context of 3D surface inspection using a laser-scanner, scan path planning is still a major challenge to obtain a complete representation of the surface in a minimum amount of time with a given scanning quality. Scan path is defined as a set of relative scanner/part configurations or driven points ensuring the quality of the acquired data according to various constraints such as visibility of the surfaces, completeness, admissible density or noise. In addition, scan path planning is even more related to other constraints like optimization of overlap and scanning time, etc. Finding the optimal strategy to scan a part, defined by its CAD model, is an issue widely addressed in the literature. Most authors base their approach on visibility and quality constraints.

Determining driven points based on the concept of visibility consists in finding the surface portions which are seen through a scanner configuration that means the surface portions that belong to the field of view (FOV) of the scanner. The field of

view is the part of the laser beam which is visible by the scanner camera. Considering the laser-scanner mounted on a CMM, Bernard and Véron propose an automatic inspection process for a complex 3D part based on three levels of visibility: local visibility, global visibility and real visibility [1]. From the CAD

model, Xi and Shu determine the optimal parameters of the scanner FOV to maximize the portion of scanned surface [2]. The surface is divided into sections by cutting the CAD model using parallel cross-sections. For each section, the optimal position is obtained by aligning the top of the FOV with the upper boundary of the surface profile. Derigent *et al.* propose to use the notion of global and local visibility through 2D visibility maps [3]. In addition to visibility, some studies propose to define driven points according to quality criteria. Prieto *et al.* [4] propose to keep the scanner normal to the surface, while following a quality criterion depending on the scanning distance and the view angle of the scanner. Mahmud *et al.* [5] build the scan path by limiting the number of orientations of the laser-scanner, and considering an optimal

digitizing distance defined as the middle of the scanner FOV. The approach developed by Lartigue *et al.* [6] relies on the representation of the part surface as a voxel map, for which the size of each voxel is defined according to the size of the scanner FOV. A unique point of view is associated to each voxel according to visibility and quality criteria. The latter are defined by admissible ranges of digitizing distances and view angles.

Wu *et al.* [7] propose a path planning method for surface inspection for a structured light scanner mounted on robot having 6 degrees of freedom. In this case, the scanner trajectory is defined as a set of discrete points of view, which must satisfy several constraints: field of view, scanning distance, scanning angle and overlap. First, a wireframe representation of the CAD model is extracted as the projection contour of the model in the main direction, which is computed by the mean of all the normal vectors in the model. Next, the model is divided into several digitizing regions using the rectangle which its dimensions are defined by the FOV of the scanner and the overlap constraint. Koutecky *et al.* [8] have recently described a method for planning scan paths of a ATOS system mounted on a KUKA robot. The surface in the form of a polygonal mesh is divided into cubes, according to the FOV and to the scanner depth of view. The driven point calculation is then carried out using the Combined Visibility Map concept. The objective is to compute the orientations of the system in order to have the greatest number of visible polygonal facets as possible. Larsson and Kjellander propose an approach for scan path planning using a laser-scanner mounted on a robot for unknown objects [9]. A first scan is made from four orthogonal directions; the scanner is positioned at the limits of the working space of the robot. From data acquired during this first scan, a shape scan step is performed to retrieve the approximate shape of the object.

Most of the methods previously detailed consider the scan path as a discrete set of points of view, which are defined according to quality and visibility constraints. Only a few studies address the issue of a continuous and smooth scan path built from the discrete points of view. Scanning overlap between 2 successive paths may alter scanning time and quality (Fig.1). Overlapping zones generally present a higher scanning noise.

Overlapping control has been more studied in relation to tool-path planning for machining or gun-path planning applied to painting using an industrial robot. In this case, the control of the overlap is essential to obtain the desired paint thickness and uniformity. Paint path planning thus presents similarities to scan path planning. In order to minimize time cycles as well as to control paint thickness uniformity, painting path strategies controlling painting overlap have been proposed in some studies [10, 11]. In their approach, Andulkar *et al.* [10] calculated the optimal overlap distance between two consecutive passes according to the distribution model of the paint. In [11], the authors show that the generation of a spray gun trajectory that uniformly covers the surface not only relies on the definition of the path orientations and the spacing between passes but also on the speed along the passes, which is not necessary in scanning.

Controlling the overlap between two successive scanning passes also presents similarities with constant scallop-height

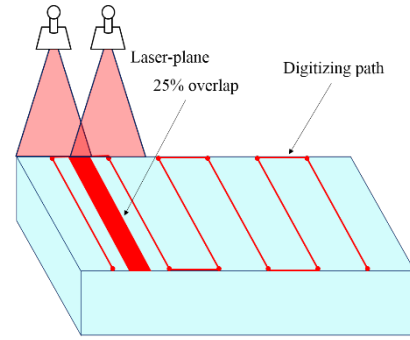


Fig.1. Definition of the overlap.

tool path methods for milling. Most methods proposed in the literature are developed for continuous surfaces [12, 13]. Some recent works propose an interesting approach more dedicated to tessellated surfaces, based on the conformal map [14, 15]. The 3D mesh surface is stretched onto a 2D plane using the conformal map. The advantage of the conformal map is to locally preserve the shape. The distances and the areas are only changed by a scaling factor [16]. Then, equidistant paths calculated in the 2D parametric space can be transformed into iso-scallop paths in 3D space by the inverse conformal map. The great advantage here is the simplification of calculation to control the overlapping, as the tool path generation is performed in the 2D space.

In this paper, we propose a method to generate a continuous scan path planning of a laser-plane scanner mounted on an industrial robot. The originality of our approach is the use of the conformal map to control the overlap between two adjacent scanning paths. Therefore, a continuous scanning path with the control of digitizing overlapping allows the management of both the orientation and the coverage rate of the laser beam. Our paper is organized as follows: our method is detailed in section 2 followed by an application in section 3. The paper ends with some concluding remarks in section 4.

## 2. Control of the digitizing overlap: ISOvScan (Iso-Overlap Scan) path method

In our approach, the digitizing system consists of a laser-plane sensor mounted on an industrial robot. The part to be digitized is represented by its tessellated CAD model. The sensor trajectory is defined as a set of ordered scanner configurations, i.e. a set of positions and orientations  $(C_E; \vec{V}_L; \vec{V}_C)$ . The position of the scanner is defined by the point  $C_E$ , which positions the scanning laser line in the field of view:  $\vec{C}_0 \vec{C}_E = d^* \cdot \vec{V}_C$ . The scanner orientation is given by the couple of vectors  $(\vec{V}_L; \vec{V}_C)$ : the director vector of the light-beam axis  $\vec{V}_L$  and the director vector of the digitizing line  $\vec{V}_L$  (Fig. 2).

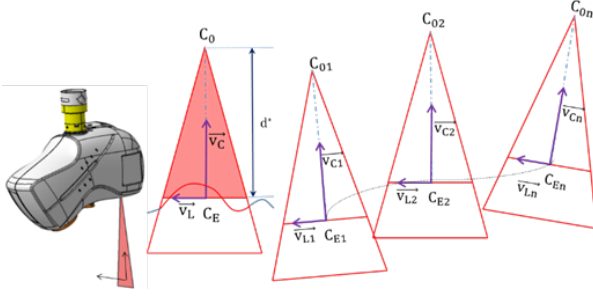


Fig.2. Parameters defining the scanner path [17].

To achieve good digitizing quality while minimizing time, we propose a continuous scanning path with the control of digitizing overlapping. The issue of finding a continuous scan path is thus to find the trajectory of  $C_E$ , and the continuous evolution of the sensor orientations defined by the couple  $(\vec{V}_L; \vec{V}_C)$  allowing the digitizing of the part. This is made possible by the use of a robot, which allows the continuous control of the sensor trajectory. On the other hand, the method to control digitizing overlap is inspired by iso-scallop tool path methods more commonly used for machining. Furthermore, to simplify calculation, the method proposes to calculate the scanner trajectory in the 2D space of the part surface, as proposed in [14]. Nevertheless, as the CAD model of the surface is not a continuous surface model but a 3D mesh, it is necessary to transform the 3D mesh surface into a 2D parametric space, using the Least-Square Conformal Map method (LSCM).

The main steps of the method we developed, called ISOvScan for Iso-Overlap Scan path, are described in the next sections. First, the 3D mesh surface is stretched on a 2D parametric surface by the LSCM method. Then, the driven points  $C_E$  of equidistant paths are generated in the 2D space, and are thus transformed in the 3D space by the inverse LSCM. For each driven point, the scanner orientations are finally calculated to satisfy quality constraints.

### 2.1. Mapping between 3D space and 2D parametric space using LSCM

First, let us introduce the LSCM method. In complex analysis, a conformal map is defined as a bijection that locally keeps the angles [17]. The transformation of a 3D triangulated surface into a 2D space  $(u, v)$  can be considered as a complex function  $\psi(s) = u(x, y) + i v(x, y)$  with  $s = x + i y$ , and  $x, y$  the coordinates in the local basis  $xy$  (Fig 3). A function is said to be conformal if it satisfies the Cauchy-Riemann conditions:

$$\frac{\partial u}{\partial x} = \frac{\partial v}{\partial y}, \quad \frac{\partial u}{\partial y} = -\frac{\partial v}{\partial x} \quad (1)$$

This method is presented in terms of simple geometric relations between the gradients in [18]. Notations are displayed in table 1.

Table 1. 3D and 2D Parameters

3D mesh parameters	2D mesh parameters
$S_T$ , set of $n$ triangular facets	$s_t$ , set of $n$ triangular facets
$T_j$ , facet $j$ , $T_j \in S_T$ , $j \in [1, n]$	$t_j$ , facet $j$ , $t_j \in s_t$ , $j \in [1, n]$

$S_v$ , set of vertices

$s_v$ : set of vertices

$V_j^k$ , vertex of the facet  $T_j$ ,  $k = 1$  to 3

$v_j^k$ , vertex of the facet  $t_j$ ,  $k = 1$  to 3

$\vec{n}_j$ , normal to facet  $T_j$

$a_{t_j}$ , area of facet  $t_j$

A facet  $T_j$ ,  $\{(x_j^1, y_j^1), (x_j^2, y_j^2), (x_j^3, y_j^3)\}$  of  $S_T$  of the surface is provided with an orthonormal basis  $xy$  (Fig. 3).

In this basis, the function which maps a point  $(x, y)$  of the triangle to a point  $(u, v)$  in the parametric space yields:

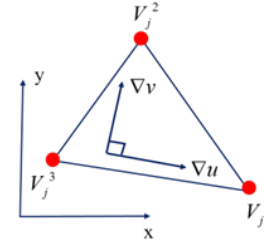


Fig.3. A triangle provided with a local  $(x, y)$  basis.

$$\begin{cases} u(x, y) = \lambda_1 u_j^1 + \lambda_2 u_j^2 + \lambda_3 u_j^3 \\ v(x, y) = \lambda_1 v_j^1 + \lambda_2 v_j^2 + \lambda_3 v_j^3 \end{cases} \quad (3)$$

where  $(\lambda_1, \lambda_2, \lambda_3)$  denote the barycentric coordinates of the point  $(x, y)$ , calculated as follows:

$$\begin{pmatrix} \lambda_1 \\ \lambda_2 \\ \lambda_3 \end{pmatrix} = \frac{1}{2|A_{T_j}|_{x,y}} \begin{pmatrix} y_j^2 - y_j^3 & x_j^3 - x_j^2 & x_j^2 y_j^3 - x_j^3 y_j^2 \\ y_j^3 - y_j^1 & x_j^1 - x_j^3 & x_j^3 y_j^1 - x_j^1 y_j^3 \\ y_j^1 - y_j^2 & x_j^2 - x_j^1 & x_j^1 y_j^2 - x_j^2 y_j^1 \end{pmatrix} \begin{pmatrix} x \\ y \\ 1 \end{pmatrix} \quad (4)$$

By substituting the values of  $(\lambda_1, \lambda_2, \lambda_3)$  in (3), this gives:

$$\nabla u = \begin{pmatrix} \partial u / \partial x \\ \partial u / \partial y \end{pmatrix} = M_{T_j} \begin{pmatrix} u_j^1 \\ u_j^2 \\ u_j^3 \end{pmatrix} \quad (5)$$

where

$$M_{T_j} = \frac{1}{2|A_{T_j}|_{x,y}} \begin{pmatrix} y_j^2 - y_j^3 & y_j^3 - y_j^1 & y_j^1 - y_j^2 \\ x_j^3 - x_j^2 & x_j^1 - x_j^3 & x_j^2 - x_j^1 \end{pmatrix} \quad (6)$$

The condition (1) can be expressed by:

$$\nabla v = \begin{pmatrix} 0 & -1 \\ 1 & 0 \end{pmatrix} \nabla u \quad (7)$$

which leads to:

$$M_{T_j} \begin{pmatrix} v_j^1 \\ v_j^2 \\ v_j^3 \end{pmatrix} - \begin{pmatrix} 0 & -1 \\ 1 & 0 \end{pmatrix} M_{T_j} \begin{pmatrix} u_j^1 \\ u_j^2 \\ u_j^3 \end{pmatrix} = \begin{pmatrix} 0 \\ 0 \end{pmatrix} \quad (8)$$

As equation (8) can only be respected for developable surfaces, for general surfaces the equation is verified in the least squares sense. Let us denote  $E_{LSCM}$  the *non-conformality* (see equation (9)). The least-squares method consists in

searching the set of parameters  $(u_j^k, v_j^k)$  which minimize  $E_{LSCM}$ .

$$E_{LSCM} = \sum_{T_j=(1,2,3)} |A_{T_j}| \left\| M_{T_j} \begin{pmatrix} v_j^1 \\ v_j^2 \\ v_j^3 \end{pmatrix} - \begin{pmatrix} 0 & -1 \\ 1 & 0 \end{pmatrix} M_{T_j} \begin{pmatrix} u_j^1 \\ u_j^2 \\ u_j^3 \end{pmatrix} \right\|^2 \quad (9)$$

After the implementation of the LSCM algorithm, a facet  $T_j$  of the 3D surface is transformed into the facet  $t_j$  in the 2D parametric space (Fig. 4). A set  $S_T$  of  $n$  triangular facets in the 3D space is then transformed into the set  $s_t$  of  $n$  triangular facets in the parametric space.

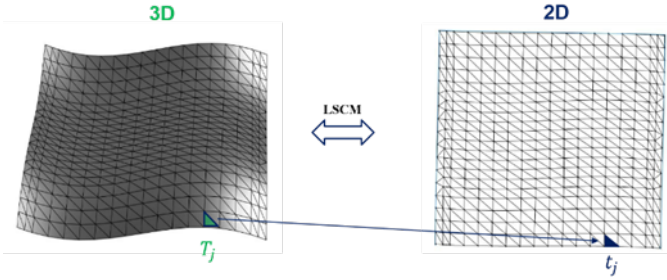


Fig.4. A 3D surface transformed into a 2D surface by LSCM.

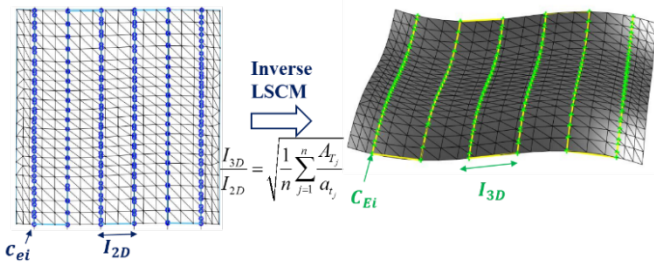


Fig.5. Interval between paths in 2D space and 3D space.

## 2.2. Generation of the scanning-path driven points

The driven points of the scan path are defined in the parametric space by the intersection between parallel planes and the parametric surface. To control the overlap, parallel planes are equidistant (Fig. 5). The displacement direction of the parallel planes is determined as the width of the rectangle that bounds the mesh in the parametric space. The interval  $I_{2D}$  between two consecutive parallel planes corresponds to the distance between two successive paths in the parametric space. The relationship between  $I_{2D}$  and the corresponding interval  $I_{3D}$ , the distance between two successive paths in the 3D space, is established considering that the ratio  $I_{3D} / I_{2D}$  is equal to the proportionality coefficient of similar triangles  $T_j$  and  $t_j$ :

$$\frac{I_{3D}}{I_{2D}} = \sqrt{\frac{1}{n} \sum_{j=1}^n \frac{A_{T_j}}{a_{t_j}}} \quad (10)$$

Therefore, when the desired interval  $I_{3D}$  is defined in order to ensure a given scanning overlap,  $I_{2D}$  is calculated using equation (10) in the parametric space. The coordinates of the driven points  $c_{ei}$  ( $c_{e1}, c_{e2}, \dots, c_{en}$ ) in the parametric space are thus obtained. As the conformal transformation is a bijective application, the inverse transformation is applied to transform

a 2D point into its corresponding 3D point. Thus, the driven point  $c_{ei}$  is transformed into  $C_{Ei}$ .

Once all driven points are calculated, the next step is to determine of the sensor orientations for each driven point. This is performed in two steps: first the vector director of the digitizing line  $\vec{V}_L$  is determined, before the light-beam axis  $\vec{V}_C$  is determined.

## 2.3. Determination of the director vector $\vec{V}_L$

In order to achieve good scanning quality for the entire surface, the digitizing distance must belong to a range of admissible values. These values are determined from the scanner assessment [19].

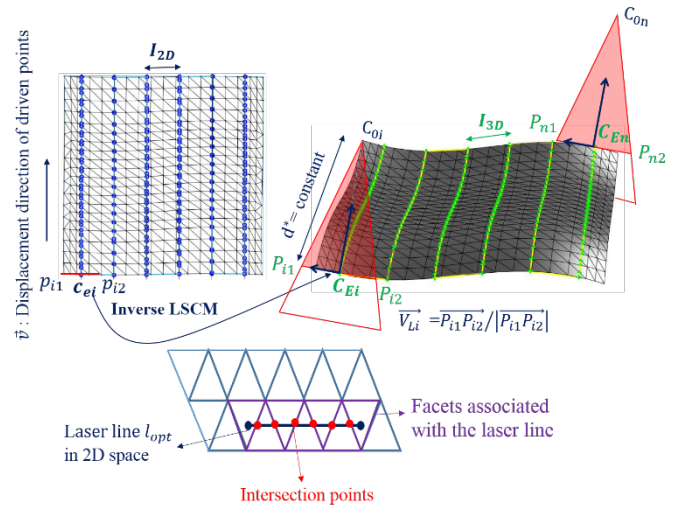


Fig.6. Determination of the scanner orientations.

A constant scanning distance is first imposed for all the driven points to ensure that the digitized surface at the driven point is visible in the FOV of the scanner, and to also ensure an expected digitizing quality. The width of the laser line, denoted  $L_{opt}$  associated to this digitizing distance is constant with respect to the scanned surface.

In order to maximize the digitized surface, the laser line must be perpendicular to the direction of displacement along the scanner trajectory in the 3D space. Then, the laser line must also be perpendicular to the direction of displacement  $\vec{v}$  of the trajectory in the 2D space. The laser-line width  $l_{opt}$  in the 2D space is defined from  $L_{opt}$  and using the proportionality coefficient:  $l_{opt} = L_{opt} / (I_{3D} / I_{2D})$ . At each point  $c_{ei}$ , the laser-line is positioned perpendicularly to the path and centered at  $c_{ei}$ . The width  $l_{opt}$  defines the two end points  $p_{i1}$  and  $p_{i2}$  of the laser line (Fig. 6). The coordinates of the corresponding points  $P_{i1}$  and  $P_{i2}$  of the points  $p_{i1}$  and  $p_{i2}$  are calculated using the LSCM inverse transformation. Thus, the director vector of the digitizing line at driven point  $C_{Ei}$  is given by:

$$\vec{V}_{Li} = \frac{P_{i1}P_{i2}}{|P_{i1}P_{i2}|} \quad (11)$$

## 2.4. Determination of director vector of light-beam axis $\vec{V}_C$

The vector of light-beam axis  $\vec{V}_C$  is determined so that the scanning direction is always perpendicular to the surface. The

facets associated to the laser line in the 2D space are also the facets associated to the laser line at the driven point in the 3D space. The normal vector to the scanned surface at the driven point  $C_{Ei}$  is calculated as the mean value of all normal vectors to the facets associated to the laser line at  $C_{Ei}$  (Fig. 6):

$$\vec{n}_{C_{Ei}} = \frac{\sum_{j=1}^{m_{C_{Ei}}} \vec{n}_j / A_{T_j}}{\left\| \sum_{j=1}^{m_{C_{Ei}}} \vec{n}_j / A_{T_j} \right\|} \quad (12)$$

where  $m_{C_{Ei}}$  is the number of facets related to the laser line at the point  $C_{Ei}$ , and  $\vec{n}_j$  is the normal vector to the facet  $j$  associated to the laser line at point  $C_{Ei}$  ( $j=1 \dots m_{C_{Ei}}$ ). Finally, the director vector of light-beam axis  $\vec{V}_C$  is defined at each driven point  $C_{Ei}$ :  $\vec{V}_{Ci} = \vec{n}_{C_{Ei}}$

The whole trajectory is thus obtained as a set of positions and orientations  $(C_{Ei}; \vec{V}_{Li}; \vec{V}_{Ci})$ . Our scan path planning method with overlap control, ISOvScan is implemented in Matlab ©.

### 3. Application

In order to assess the ISOvScan method, an application is proposed using the scanning system which consists of a laser-plane scanner Zephyr II ([www.kreon3d.fr](http://www.kreon3d.fr)) mounted on an industrial Mitsubishi robot and an optical tracker (Fig. 7). This system provides an independent measurement of the scanner positions.

First, a protocol of scanner assessment is applied to identify the actual scanner parameters such as the dimensions of the FOV, and the admissible ranges of scanning distances which decide the scanning quality.

#### 3.1. Scanner parameters

The dimensions of the FOV of the scanner Zephyr II are identified by measuring a reference plane. Considering the laser-line as the intersection between the reference plane and the laser-beam, the depth  $H$  corresponds to the height of the FOV, for which the laser-line is visible in the CCD. The value of  $H$  given by the experiment is  $115 \text{ mm}$ . According to the QUALIPSO protocol detailed in [19], we can determine that the minimum value of noise corresponds to the digitizing distance  $d^* = 60 \text{ mm}$  from the top of the FOV, giving the laser-line width  $L_{opt} = 77 \text{ mm}$ . This digitizing distance is therefore used for the experiment.

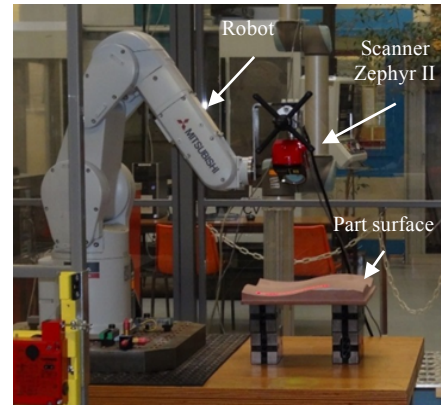
The choice of the overlap value must result from a compromise between the number of paths and the scanning noise. Experiments, performed by measuring a reference plane with various percentages of overlap, have highlighted that the percentage of overlap should be lesser than 25% to optimize the number of paths. Experiments also bring out that the noise strongly increases when overlap is greater than 15%. Therefore, the selected value for the overlap is 15%, which fixes the value of  $I_{3D}$ , considering the linewidth.

#### 3.2. Experiments

The method is applied on the part proposed in Fig. 8, using the parameters previously selected. The resulting scan path is reported in Fig. 8.

The scan path is first assessed by a simulator previously developed [20]. This simulator relies on the analysis of scanner configurations relatively to the studied part. Green color corresponds to well-facets digitized (admissible range of scanning distances and view angles), yellow for the facets in the overlap zones (Fig. 9).

The proposed method ISOvScan is thus tested by using the industrial robot equipped with the optical tracker system, which acquires the scanner's positions in an independent frame. Point cloud acquisition is achieved thanks to Kreon Polygonia software. Prior to the execution, the robot displacements are simulated using RoboDK from the scan path issued from ISOvScan, to assess the consistency of the trajectory in the



robot coordinate system.

Fig.7. Scanning system.

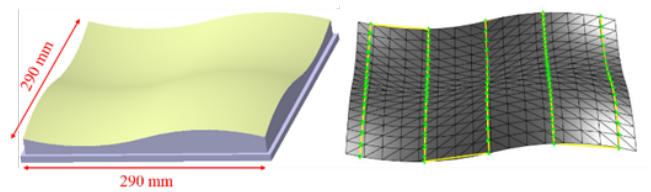


Fig.8. CAD model (left); Scan path (right).

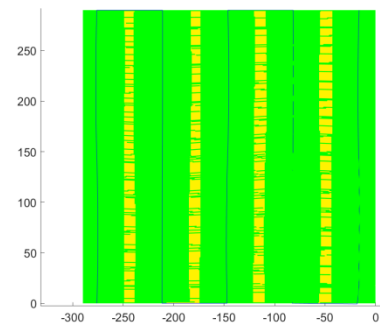


Fig.9. Result of the scanning simulation.

### 3.3. Results and discussion

The scanning gives a set of 1 629 604 points. The point cloud obtained after digitizing is compared to the part CAD model in order to identify geometrical deviations. The comparison, performed using the open source software *CloudCompare*, shows that the main deviations are located at one border of the surface, which is likely due to the measuring conditions. There are also digitizing holes on the surface (Fig. 10) caused by the instability of laser beam, which disappears for several seconds during the scanning process for unexplained technological reasons.

To evaluate the digitizing noise, the point cloud is registered with the nominal mesh surface. The set of digitized points belonging to the cylinder so defined corresponds to the actual digitized facet. For each facet, the distances between the digitized points and the facet are calculated. The associated standard deviation represents the actual digitizing noise. Results are displayed in Fig. 11, in which the scale of colours accounts for the digitizing noise evolution.

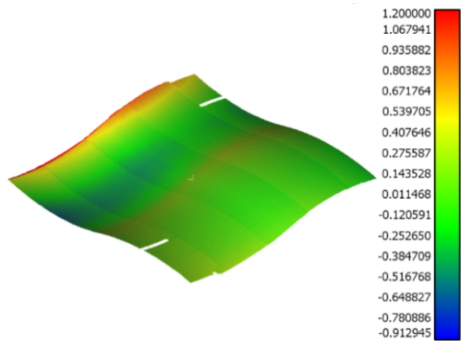


Fig.10. Geometrical deviations (mm) between point cloud and CAD model.

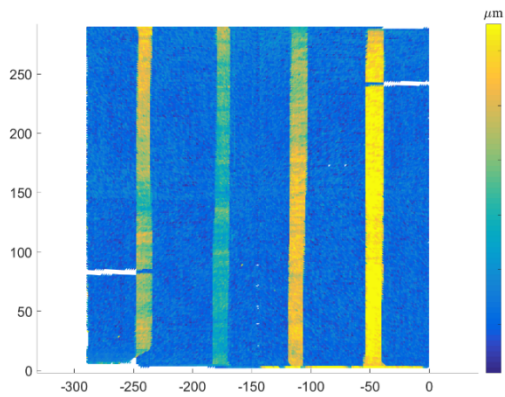


Fig.11. Evolution of digitizing noise on the surface.

Results clearly highlight the effect of the overlap. Indeed, point density for overlap zones is higher than for other zones, and as a result, digitizing noise in overlap zones is always greater than for non-overlap zones. This result emphasizes how important the overlap control in scan path generation is. It also assesses the good of efficiency of ISOvScan for scan path planning with the control of overlap.

### 4. Conclusion

In this paper we have proposed a new method of scan path planning for automated inspection of manufactured part using an industrial robot, based on the control of the overlap between 2 successive scanning paths. A continuous scanning path with the control of the overlap can control the orientation and the coverage rate of the laser beam. Therefore, digitizing quality as well as digitizing time can be controlled by optimizing overlapping zones. Nevertheless, the generated scan path has some limitations. Since the driven points are created from the intersection between the equidistant planes and the facets of the surface in 2D space, there is sudden change of scanner orientation when the scanner moves from one point to another. This may cause undesirable noise in some areas on the surface.

Future work will concentrate on smoothing out the scan path obtained from ISOvScan by spline interpolation. This spline scan path will be better adapted to the robot motion control.

### Acknowledgements

This research was made possible by the equipment support from Kreon Technology. We gratefully acknowledge the help provided by Mr. Tom Ranger and Mr. Dorian Verdel for their technical assistance in our experimental work.

### References

- [1] Bernard A and Véron M. Visibility theory applied to automatic control of 3d complex parts using plane laser sensors. *CIRP Annals - Manufacturing Technology* 2000; vol. 49, no. 1, pp. 113 – 118.
- [2] Xi F and Shu C. Cad-based path planning for 3-d line laser scanning. *Computer-Aided Design* 1999; vol. 31, no. 7, pp. 473–479.
- [3] Derigent W, Remy S, and Ris G. A new approach of the visibility calculation of an object. *International journal of manufacturing technology and management* 2004; vol. 6, no. 6, pp. 550–556.
- [4] Prieto F, Redarce H, Lepage R, and Boulanger P. Range image accuracy improvement by acquisition planning. *Proceedings of the 12th conference on vision interface 1999, Trois Rivieres, Québec, Canada*, pp. 18–21.
- [5] Mahmud M, Joannic D, Roy M, Isheil A, and Fontaine J.-F. 3D part inspection path planning of a laser scanner with control on the uncertainty. *Computer-Aided Design* 2001 vol. 43, no. 4, pp. 345–355.
- [6] Lartigue C, Quinsat Y, Mehdi-Souzani C, Zuquete-Guarato A, and Tabibian S. Voxel-based path planning for 3d scanning of mechanical parts. *Computer-Aided Design and Applications* 2014; vol. 11, no. 2, pp. 220–227.
- [7] Wu Q, Lu J, Zou W, and Xu D. Path planning for surface inspection on a robot-based scanning system. *IEEE International Conference on Mechatronics and Automation (ICMA)* 2015, pp. 2284–2289.
- [8] Koutecky T, Palousek D, and Brandejs J. Sensor planning system for fringe projection scanning of sheet metal parts. *Measurement* 2016; vol. 94, pp. 60–70.
- [9] Larsson S and Kjellander J. A. Path planning for laser scanning with an industrial robot. *Robotics and Autonomous Systems* 2008; vol. 56, no. 7, pp. 615–624.
- [10] Andulkar M. V, Chiddarwar S. S, and Marathe A. S. Novel integrated offline trajectory generation approach for robot assisted spray painting operation. *Journal of Manufacturing Systems* 2015; vol. 37, pp. 201–216.
- [11] Atkar P. N, Conner D. C, Greenfield A, Choset H, and Rizzi A. A. Uniform coverage of simple surfaces embedded in R3 for auto-body painting. In *Algorithmic Foundations of Robotics VI*, pp. 27–42, Springer 2004.
- [12] Tournier C and Duc E. A surface based approach for constant scallop height tool-path generation. *The International Journal of Advanced Manufacturing Technology* 2002; vol. 19, no. 5, pp. 318–324.
- [13] Can A and Ünüvar A. A novel iso-scallop tool-path generation for efficient five-axis machining of free-form surfaces. *The International Journal of Advanced Manufacturing Technology* 2010; vol. 51, no. 9–12, pp. 1083–

- [14] Li W, Yin Z, Huang Y, Wu T, and Xiong Y. Tool path generation for triangular meshes using least-squares conformal map. *International journal of production research* 2011; vol. 49, no. 12, pp. 3653–3667.
- [15] Zhao J, Zou Q, Li L, and Zhou B. Tool path planning based on conformal parameterization for meshes. *Chinese Journal of Aeronautics* 2015; vol. 28, no. 5, pp. 1555–1563.
- [16] Haker S, Angenent S, Tannenbaum A, Kikinis R, Sapiro G, and Halle M. Conformal surface parameterization for texture mapping. *IEEE Transactions on Visualization and Computer Graphics* 2000; vol. 6, no. 2, pp. 181–189.
- [17] Lévy B, Petitjean S, Ray N, and Maillot J. Least squares conformal maps for automatic texture atlas generation. *ACM Transactions on Graphics (TOG)* 2002; vol. 21, no. 3, pp. 362–371.
- [18] Hormann K, Lévy B, and Sheffer A. *Mesh parameterization: Theory and practice*. SIGGRAPH Course Notes, 2007.
- [19] Mehdi-Souzani C, Quinsat Y, Lartigue C, and Bourdet P. A knowledge database of qualified digitizing systems for the selection of the best system according to the application. *CIRP Journal of Manufacturing Science and Technology* 2016; vol. 13, pp. 15–23.
- [20] Phan N. D. M, Quinsat Y, and Lartigue C. Simulation of laser-sensor digitizing for on-machine part inspection. *Advances on Mechanics, Design Engineering and Manufacturing*, pp. 301–311, Springer, 2017.